

Postprint of: Litzbarski L., Klimczuk T., Winiarski M., Synthesis, structure and physical properties of new intermetallic spin glass-like compounds RE_2PdGe_3 ($RE = Tb$ and Dy), *JOURNAL OF PHYSICS-CONDENSED MATTER*, Vol. 32, iss. 22 (2020), 225706, DOI: [10.1088/1361-648X/ab73a4](https://doi.org/10.1088/1361-648X/ab73a4)

Synthesis, structure and physical properties of new intermetallic spin glass-like compounds

RE_2PdGe_3 ($RE = Tb$ and Dy)

L.S. Litzbarski, T. Klimczuk, M.J. Winiarski

Faculty of Applied Physics and Mathematics, Gdansk University of Technology,

Narutowicza 11/12, 80-233 Gdansk, Poland

Abstract

New intermetallic compounds $Tb_2Pd_{1.25}Ge_{2.75}$ and $Dy_2Pd_{1.25}Ge_{2.75}$ have been synthesized using the arc-melting method. The crystallographic structure and magnetic, electronic transport, and thermal properties are reported. The crystal structure obtained from powder X-ray diffraction analysis suggests that these compounds crystallize in the AlB_2 -type structure (space group $P6/mmm$, no. 191) with lattice parameters $a = 4.22853(5) / 4.23054(2) \text{ \AA}$ and $c = 3.94225(9) / 3.94552(5) \text{ \AA}$ for the compounds with Tb and Dy respectively. The ac and dc magnetic susceptibility studies reveal spin-glass like behavior, with freezing temperature $T_f = 10.5 \text{ K}$ for $Tb_2Pd_{1.25}Ge_{2.75}$ and 4.5 K for $Dy_2Pd_{1.25}Ge_{2.75}$. These data are in good agreement with the heat capacity measurements.

Introduction

During the last few years, several compounds of the type RE_2TGe_3 , where RE is a rare earth element and T is a transition metal, have been studied. These compounds have a crystal structure derived from that of AlB_2 and show interesting physical properties. For example Y_2PdGe_3 [1] is a superconductor with $T_c = 3 \text{ K}$ and Gd_2PdGe_3 exhibits antiferromagnetic order below 10 K [2].

Most of the reported intermetallic compounds in the RE_2PdGe_3 family crystallize in the hexagonal ($P6/mmm$) structure [1-4]. The hexagonal AlB_2 type structure represents one of the simplest inorganic structure types, with the unit cell consisting of only three atoms. The AlB_2 structure is composed of alternating hexagonal layers of Al and graphite-like honeycomb layers of B , as shown in Fig. 1 (a) and (b) (all crystal structure drawings were produced using the VESTA program [5]). These boron layers are well separated from each other ($d_{inter} = c \approx 3.3 \text{ \AA}$) and the distance between contiguous boron atoms is defined by the lattice parameter a : $d_{intra} = a/\sqrt{3} \approx 1.7 \text{ \AA}$. It is possible to get AlB_2 -related structures by substitution of aluminum atoms with a rare earth or actinoid metal and replacing boron by silicon or germanium, which generates a large family of binary compounds. In ternary compounds the hexagonal layer is made up of a transition metal and a main group element. Such compounds exist in two types of $P6/mmm$ structure: the ordered variant, presented in Fig. 1(c), characterized by a lattice parameter ratio $c/a \approx 0.5$ (e.g. Ca_2PdGe_3) [6], and the disordered variant, which is shown in Fig 1(d), with c/a about 1.

We have searched for new materials with long range magnetic ordering in the $RE(\text{Pd}, \text{Ge})_2$ family and succeeded in the synthesis of spin-glass like $\text{Tb}_2\text{Pd}_{1.25}\text{Ge}_{2.75}$ and $\text{Dy}_2\text{Pd}_{1.25}\text{Ge}_{2.75}$. In this paper, we describe synthesis, crystal structure and physical properties of these compounds.

Experimental

The synthesis of $RE_2\text{Pd}_{1+x}\text{Ge}_{3-x}$ ($x = 0 - 0.35$) was performed using an arc-melting method. Stoichiometric amounts of palladium (99.95%, Alfa Aesar) and germanium (99.999%, Alfa Aesar) were weighted. Due to the volatility of terbium (99.9%, Onyxmet) and dysprosium (99.9%, Onyxmet), these chemical elements were used in 2% molar excess. The mixture of Tb or Dy, Pd and Ge was melted together under a high purity, Zr-gettered, argon atmosphere in an arc furnace (MAM-1 GmbH Edmund Bühler). The polycrystalline ingot was turned several times to ensure homogeneity. The total weight losses during the melting process were less than 0.5%.

The samples were characterized by powder X – ray diffraction obtained employing a Bruker D2Phaser diffractometer with CuK_α radiation, equipped with a XE-T detector. The results were processed by means of LeBail refinement using the FullProf software [7]. $\text{Tb}_2\text{Pd}_{1.25}\text{Ge}_{2.75}$ was also examined by EDS spectroscopy using a scanning electron microscope FEI Quanta FEG 250 to confirm the chemical composition of the obtained samples.

Samples of $\text{Tb}_2\text{Pd}_{1.25}\text{Ge}_{2.75}$ and $\text{Dy}_2\text{Pd}_{1.25}\text{Ge}_{2.75}$ were investigated by heat capacity, electrical transport and magnetic measurements using a Quantum Design Physical Property Measurement System (PPMS). The electrical resistivity measurements were performed using a standard four probe technique with an applied current of 5 mA. Electrical contacts were made by spot-welding platinum wires ($\phi = 50 \mu\text{m}$) on the sample surface. Magnetization was measured with various magnetic fields after field cooling (FC) and zero field cooling (ZFC). In the case of AC measurement of magnetic susceptibility, the AC Measurement System (ACMS) was used. Susceptibility was approximated as sample magnetization divided by the applied magnetic field: $\chi \approx M/H$. Time evolution of magnetization was measured in ZFC mode, in which the sample is initially cooled down to relevant temperature and next a small amount of magnetic field is applied to start recording $M(t)$ data. The heat capacity data were obtained by using the thermal relaxation technique in the temperature range $1.9 \text{ K} < T < 300 \text{ K}$.

Results and discussion

Synthesized samples of $RE_2\text{Pd}_{1+x}\text{Ge}_{3-x}$ were investigated by powder X- ray diffraction (XRD). It was observed that for $x = 0.25$ samples were single-phase, while in other cases they were contaminated by a parasitic phase of 1:2:2 stoichiometry (ThCr₂Si₂ type structure). The sample of $\text{Tb}_2\text{Pd}_{1.25}\text{Ge}_{2.75}$ was studied by EDS spectroscopy and the average composition of the pellet is within an error of the

nominal composition. XRD patterns (Fig. 2) confirmed that $\text{Tb}_2\text{Pd}_{1.25}\text{Ge}_{2.75}$ crystallizes in the AlB_2 -type hexagonal structure. Unlike Ca_2PdGe_3 [6], $\text{Tb}_2\text{Pd}_{1.25}\text{Ge}_{2.75}$ shows no superstructure reflections, suggesting a statistical disorder within the Pd-Ge plane. The same observation had been made for $\text{Dy}_2\text{Pd}_{1.25}\text{Ge}_{2.75}$. Structural parameters, which were calculated by Le Bail refinements, are gathered in Table 1. Received values are close to those for Gd_2PdGe_3 [2], Nd_2PdGe_3 and Y_2PdGe_3 [3]. It can be observed that the volume of a unit cell is growing with the increase of the atomic radius of the rare earth metal in RE_2PdGe_3 compounds.

An anisotropic broadening effect was observed in the XRD pattern, the $00l$ reflections being far more broadened than others. This may suggest a presence of stacking faults in the structure, the anisotropic strain distribution, or a combination of both. In order to improve the LeBail fit, the effect was modelled using the quartic model of anisotropic strain implemented in Fullprof [8].

Fig. 3 shows the temperature dependence of magnetic susceptibility measured at $\mu_0H = 0.1$ T for (a) $\text{Tb}_2\text{Pd}_{1.25}\text{Ge}_{2.75}$ and (b) $\text{Dy}_2\text{Pd}_{1.25}\text{Ge}_{2.75}$. $\chi(T)$ increases with decreasing temperature, which is typical behavior for Curie–Weiss paramagnets. Plots of inverse magnetic susceptibility versus temperature are shown in insets. The plot for the sample containing dysprosium is linear in the range $T = 25$ -300 K, and thus it is fitted with a dependence formulated with the Curie-Weiss law in this range. The plot of inverse of χ versus T for the compound with terbium is found to be linear above 50 K and it is also fitted with a Curie – Weiss law. Obtained values of the paramagnetic Curie temperature (θ_{cw}) and Curie constant (C) are gathered in Table 2. The effective magnetic moment was calculated using equation:

$$\mu_{\text{eff}} = \left(\frac{3Ck_B}{\mu_B^2 N_A} \right)^{1/2},$$

where k_B is the Boltzmann constant, μ_B is the Bohr magneton and N_A is the Avogadro number. The resulting μ_{eff} is slightly larger than theoretical value for Tb^{3+} free ion ($9.72 \mu_B$) [9], which may be caused by a small magnetic moment induced on Pd. In the case of $\text{Dy}_2\text{Pd}_{1.25}\text{Ge}_{2.75}$ the calculated value of the effective magnetic moment is close to the theoretical value for Dy^{3+} ($10.65 \mu_B$) [9], which is consistent with the trivalent nature of the dysprosium ion. The low temperature FC and ZFC magnetization of the Tb compound deviate below $T = 12$ K (Fig. 4(a)). The transition temperature (T_T) is obtained as a maximum of $d(\chi T)/dT$ for $\mu_0H = 100$ Oe, and is equal to $T_T = 10.5$ K. This value is close to the ordering temperature for Gd_2PdGe_3 ($T_T = 10$ K) [2]. The transition temperature for $\text{Dy}_2\text{Pd}_{1.25}\text{Ge}_{2.75}$ is estimated in the same way. It can be observed that the value of T_T shifts to lower temperatures with increasing H . Moreover, the value of T_T obtained from plot in Fig. 4(b) is more than twice as small as for $\text{Tb}_2\text{Pd}_{1.25}\text{Ge}_{2.75}$ ($T_T = 4.5$ K). The inset of Fig. 4(a) displays the field dependence of $M(H)$ at $T = 2$ K for $\text{Tb}_2\text{Pd}_{1.25}\text{Ge}_{2.75}$. It is obvious that the magnetization curve does not saturate, even at the highest applied field ($\mu_0H = 9$ T). This phenomenon can be explained by the absence of long-range magnetic ordering, which agrees with spin–glass like character of $\text{Tb}_2\text{Pd}_{1.25}\text{Ge}_{2.75}$. A



similar effect can be observed for $\text{Dy}_2\text{Pd}_{1.25}\text{Ge}_{2.75}$ (inset of Fig. 4(b)). Both compounds show a well-defined peak of $\chi(T)$ at low temperatures, which looks similar to the typical temperature dependence of the susceptibility for an antiferromagnetic material [10]. However, for a non-frustrated magnet the value of $|\theta_{\text{CW}}|$ is comparable to T_{N} . Both $\text{Tb}_2\text{Pd}_{1.25}\text{Ge}_{2.75}$ and $\text{Dy}_2\text{Pd}_{1.25}\text{Ge}_{2.75}$ have transition temperatures approximately three times smaller than $|\theta_{\text{CW}}|$. The empirical measure of frustration ($f = |\theta_{\text{CW}}|/T_{\text{T}}$) is much larger than 1 in both cases, suggesting magnetic frustration [11]. This feature, together with Pd-Ge site disorder and the possible presence of stacking faults, suggests that both compounds are spin-glass like materials and thus the observed magnetization drop below T_{T} results from a spin-freezing transition.

To confirm this hypothesis, measurements of the time-dependent remnant magnetization in the isothermal process for $\text{Tb}_2\text{Pd}_{1.25}\text{Ge}_{2.75}$ and $\text{Dy}_2\text{Pd}_{1.25}\text{Ge}_{2.75}$ were performed (Fig. 5 (a) and (b) respectively). The time evolution of the magnetization resulting from slow relaxation is observed for both samples for T below freezing temperature. This behavior is known as the ageing effect and it is one of the crucial features in spin – glass like materials [12, 13, 14, 15]. Obtained curves may be fitted by the logarithmic function of time: $M(t) = M_0 + S \ln(t/t_0 + 1)$, where M_0 is magnetization at $t = 0$ and S is the magnetic viscosity. The reference time t_0 depends on the measuring conditions and has only limited physical relevance [12, 14]. The best fitting results obtained by using the least-squares method are shown by solid lines in Fig. 5. Estimated values of the zero-field magnetization and magnetic viscosity are collected in Table 2. These values are comparable to the ones reported for other spin – glass like compounds [12, 13, 14, 15]. Another important feature of spin – glass like behavior is shown in Fig. 6: the real part of the ac magnetic susceptibility exhibits a strong dependency of the magnetic transition on the frequency of the ac excitation field. The ac magnetic susceptibility was measured at frequencies $\nu = 19, 66, 233, 816, 2856$ and 10000 Hz (logarithmic spacing) at an applied dc magnetic field $H_{\text{dc}} = 5$ Oe with $H_{\text{ac}} = 3$ Oe ac excitations, in a temperature range $T = 10\text{--}16$ K and $T = 4\text{--}8$ K for $\text{Tb}_2\text{Pd}_{1.25}\text{Ge}_{2.75}$ and $\text{Dy}_2\text{Pd}_{1.25}\text{Ge}_{2.75}$, respectively. In both cases the maximum in M' increases and shifts towards lower temperature as the frequency of the excitation field is decreased. The frequency (ν) dependence of the freezing temperature can be described by the empirical Vogel-Fulcher law:

$$T_f = T_0 - \frac{E_a}{k_B} \frac{1}{\ln(\tau_0 \nu)},$$

with three fitting parameters: activation energy E_a (k_B is the Boltzman constant), Vogel – Fulcher temperature T_0 and intrinsic relaxation time τ_0 [15, 16]. The last of these parameters can vary from $\tau_0 = 10^{-7}$ s for cluster glass compounds to $\tau_0 = 10^{-13}$ s for spin – glass materials. The best fitting results for samples with terbium and dysprosium were obtained for $\tau_0 = 10^{-11}$ s, which is shown in a plot of the freezing temperature versus $1/\ln(\tau_0 \nu)$ (insets of Fig. 6). The calculated values of activation energy are equal to $5.88 k_B T_f$ and $8.58 k_B T_f$ for terbium and dysprosium samples respectively and are presented in

Table 2. These values are about two times smaller than in the case of the silicon analogs RE_2PdSi_3 ($RE = Tb, Dy$), but still have an order of magnitude that is typical for spin – glass materials [15].

Heat capacity (C_p) measurements for $Tb_2Pd_{1.25}Ge_{2.75}$ and $Dy_2Pd_{1.25}Ge_{2.75}$ are shown in Fig. 7. In both cases at room temperature C_p reaches the expected Dulong-Petit law value, $3nR \approx 150 \text{ J mol}^{-1} \text{ K}^{-1}$, where n is the number of atoms per formula unit ($n = 6$) and R is the gas constant ($R = 8.314 \text{ J mol}^{-1} \text{ K}^{-1}$). The insets of Fig. 7 show the dependence of C_p/T at low temperatures. Both samples have a well-defined upturn at about the freezing temperature, which confirms that $RE_2Pd_{1.25}Ge_{2.75}$ ($RE = Tb, Dy$) can be classified as spin-glass like materials. In both cases the C_p peak is only weakly affected by the applied magnetic field.

The temperature dependence of the electrical resistivity (ρ) for $Tb_2Pd_{1.25}Ge_{2.75}$ is presented in Fig 8. For temperatures above $T = 75 \text{ K}$, $\rho(T)$ weakly decreases and exhibits the expected metallic behavior without any other noteworthy features. As the temperature decreases further, the electrical resistivity goes through cusps, which can be interpreted as a reduction of spin disorder scattering upon a magnetic transition. This feature is also observed in other compounds of the RE_2PdGe_3 family ($RE = Ce, Nd, Gd$) [2,3,18]. However, the value of transition temperature for $\rho(T)$ (the inset of Fig. 8) does not agree with that obtained from magnetization and heat capacity measurements, likely because there is no long-range spatial correlation function due to the lack of a periodically ordered state. This would suggest that disorder near the freezing temperature, still has a significant contribution to the electron scattering [19]. The calculated value of the residual resistivity ratio ($RRR = \rho_{(300 \text{ K})}/\rho_{(2 \text{ K})}$) is 1.1, which is typical for polycrystalline samples with internal defects or disorder. The magnetoresistance, which is defined as $MR = [\rho(H) - \rho(0)]/\rho(0)$ was measured as a function of magnetic field at selected temperatures near the freezing temperature for $Tb_2Pd_{1.25}Ge_{2.75}$ sample (Fig. 9). The sign of the magnetoresistance is negative and is varying approximately quadratically with the applied magnetic field for a wide range temperatures above the freezing temperature, which is expected for a state with a dominance of paramagnetic fluctuations [20]. Below T_f a qualitative change of the $MR(H)$ plot can be observed. This behavior was also reported for Nd_2PdGe_3 [3] and is likely caused by the decrease in spin-disorder scattering upon a magnetic transition, which is suppressed by an applied magnetic field.

Conclusions

We have synthesized polycrystalline samples of new intermetallic compounds $Tb_2Pd_{1.25}Ge_{2.75}$ and $Dy_2Pd_{1.25}Ge_{2.75}$ by an arc melting technique. Powder X-ray diffraction confirms that these compounds crystallize in a hexagonal structure ($P6/mmm$), a disordered variant of AlB_2 type, with refined lattice parameters $a = 4.22853(5) \text{ \AA}$, $c = 3.94225(9) \text{ \AA}$ and $a = 4.22548(2) \text{ \AA}$, $c = 3.90381(5) \text{ \AA}$, for the Tb and Dy compounds respectively. The temperature dependence of the magnetic susceptibility obeys the Curie – Weiss law in the high temperature region for both compounds. The ac susceptibility and

magnetic relaxation measurements give evidence for the formation of a spin – glass like state in $\text{Tb}_2\text{Pd}_{1.25}\text{Ge}_{2.75}$ and $\text{Dy}_2\text{Pd}_{1.25}\text{Ge}_{2.75}$ with freezing temperatures $T_f = 11.5$ K and $T_f = 4.5$ K respectively. These results are in good agreement with data obtained from heat capacity measurements. The temperature dependence of the electrical resistivity for the Tb compound shows metallic character. The low value of $\text{RRR} = 1.1$ is in agreement with the Pd-Ge site disorder.

Acknowledgments

This work was supported by Ministry of Science and Higher Education (Poland) under project 0142/DIA/2018/47 (“Diamentowy Grant”). M.J. Winiarski is supported by the Foundation for Polish Science (FNP).

References

- [1] E.V Sampathkumaran, S. Majumdar, W. Schneider, S.L. Molodtsov, C. Laubschat, Superconductivity in Y_2PdGe_3 , *Physica B*, 312-313 (2002) 152-154
- [2] S. Majumdar, M.M Kumar, E.V. Sampathkumaran, Magnetic behavior of new compound Gd_2PdGe_3 , *J. Alloy. Compd.* 288(1) (1999) 61-64
- [3] S. Majumdar and E.V Sampathkumaran, Observation of enhanced magnetic transition temperature in Nd_2PdGe_3 and superconductivity in Y_2PdGe_3 , *Phys. Rev. B*, 63 (2001) 172407
- [4] Yu.D. Seropegin, O.L. Borisenko, O.I. Bodak, V.F. Nikiforov, M.V. Kovachikova, Yu.V. Kochetkov, Investigation of phase relationship and physical properties of Yb_Pd_Ge compounds, *J. Alloy. Compd.* 216 (1994) 259-263
- [5] K. Momma, F. Izumi, VESTA 3 for three – dimensional visualization of crystal, volumetric and morphology data, *J. Appl. Crystallogr.* 44 (6) (2011) 1272 - 1276
- [6] T. Klimczuk, Weiwei Xie, M.J. Winiarski, R. Koziol, L.S. Litzbarski, Huixia Luo, R.J. Cava, Crystal structure and physical properties of new Ca_2TGe_3 (T=Pd and Pt) germanides, *J. Solid State Chem.* 243 (2016) 95-100
- [7] J. Rodriguez-Carvajal, Recent advances in magnetic structure determination by neutron powder diffraction, *Physica B*192 (1993) 55-69
- [8] J. Rodriguez-Carvajal, T. Roisnel, Line broadening analysis using Fullprof*: determination of microstructural properties, *Materials Science Forum* 443-444 (2004) 123-126
- [9] J. Jensen, A. Mackintosh, Rare Earth Magnetism: Structures and Excitations, Clarendon Press, 1991
- [10] N.A. Spaldin, Magnetic Materials: Fundamentals and Applications, Cambridge University Press, 2011
- [11] A.P. Ramirez, Strongly geometrically frustrated magnets, *Annu. Rev. Mater. Sci.* 24:453-80 (1994)
- [12] Hu Guang-Hui, Li Ling-Wei, I. Umehara, Pressure effect on magnetic phase transition and spin-glass-like behavior of $GdCo_2B_2$, *Chinese Physics B*, 2016, 25(6): 067501
- [13] S. Sarkar, A. Mondal, N. Giri and R. Ray, Spin glass like transition and the exchange bias effect in Co_3O_4 nans anchored onto graphene sheets, *Phys. Chem. Chem. Phys.*, 2019,21,260
- [14] S. Harikrishnan, S. Rößler, C.M.N Kumar, Y. Xiao, H.L. Bhat, U.K. Rößler, F. Steglich, S. Wirth, Suja Elizabeth, Memory effect in $Dy_{0.5}Sr_{0.5}MnO_3$ single crystals, *J. Phys.: Condens. Matter* 22 (2010) 3460002
- [15] D.X. Li, S. Nimori, Y. Shiokawa, Y. Haga, E. Yamamoto, Y. Onuki, ac susceptibility and magnetic relaxation of R_2PdSi_3 , *Phys. Rev. B* 68, 012413 (2003)
- [16] K. Górnicka, K.K. Kolincio, T. Klimczuk, Spin- glass behavior in a binary Pr_3Ir intermetallic compound, *Intermetallics* 100 (2018) 63-69
- [17] T. Klimczuk, H.W. Zandbergen, Q. Huang, T.M. McQueen, F. Ronning, B. Kusz, J.D. Thompson, R.J. Cava, Cluster – glass behavior of highly oxygen deficient perovskite $BaBi_{0.28}Co_{0.72}O_{2.2}$, *J. Phys Condens Matter* 21 (2009) 105801

[18] R.E. Baumbach, A. Gallagher, T. Besara, J. Sun, T. Siegrist, D.J. Singh, J.D. Thompson, F. Ronning and E.D. Bauer, Complex magnetism and strong electronic correlations in Ce₂PdGe₃, Phys. Rev. B 91, 035102 (2015)

[19] J.A. Mydosh, Spin glasses: an experimental introduction, Taylor & Francis, London, 1993

[20] MK Chattopadhyay, P. Arora, S.B. Roy, The magnetotransport properties of the intermetallic compound GdCu₆, J. Phys. Condens. Matter, 24(14):146004, 2012

Tables

Table 1

Refined structural parameters for $\text{Tb}_2\text{Pd}_{1.25}\text{Ge}_{2.75}$ and $\text{Dy}_2\text{Pd}_{1.25}\text{Ge}_{2.75}$

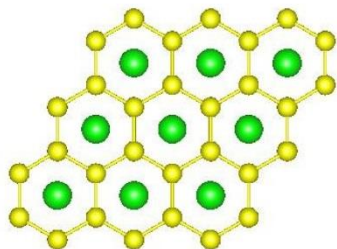
Refined Formula	$\text{Tb}_2\text{Pd}_{1.25}\text{Ge}_{2.75}$	$\text{Dy}_2\text{Pd}_{1.25}\text{Ge}_{2.75}$
Space group	<i>P6/mmm</i> (No.191)	
<i>a</i> (Å)	4.22605(6)	4.23048 (5)
<i>c</i> (Å)	3.90458(11)	3.94526(8)
<i>V</i> (Å ³)	60.391(2)	61.149(2)
Molar weight (g mol ⁻³)	657.78	650.63
Density (g cm ³)	5.44	5.32
Tb (1a)	x = y = z = 0	
Pd (2d)	x = 1/3 y = 2/3 z = 0.5	
Ge (2d)	x = 1/3 y = 2/3 z = 0.5	
Figures of merit:		
R _p (%)	10.2	8.70
R _{wp} (%)	10.6	9.67
R _{expt} (%)	6.11	5.73
χ ²	3.01	2.91

Table 2Selected physical property data for $\text{Tb}_2\text{Pd}_{1.25}\text{Ge}_{2.75}$ and $\text{Dy}_2\text{Pd}_{1.25}\text{Ge}_{2.75}$

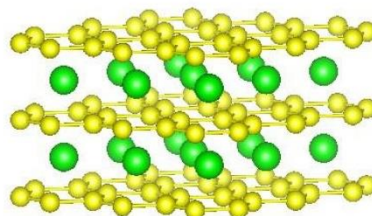
	$\text{Tb}_2\text{Pd}_{1.25}\text{Ge}_{2.75}$	$\text{Dy}_2\text{Pd}_{1.25}\text{Ge}_{2.75}$
T_f (K)	10.5	4.5
f	2.7	3.0
E_a/k_B (K)	67.6(9)	38.6(9)
T_0 (K)	7.74(7)	3.10(7)
Θ_{CW} (K)	-27.28(14)	-13.23(3)
μ_{Eff} (μ_B)	10.69	10.79
M_0 (emu/g)	0.8311(8)	2.111(3)
S (emu/g)	0.0068(3)	0.0148(4)
RRR	1.1	-

Figures

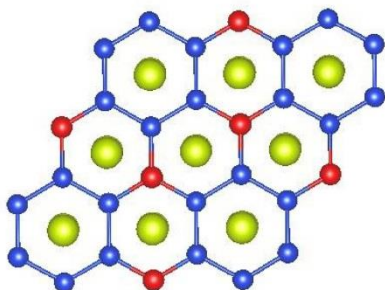
a)



b)



c)



d)

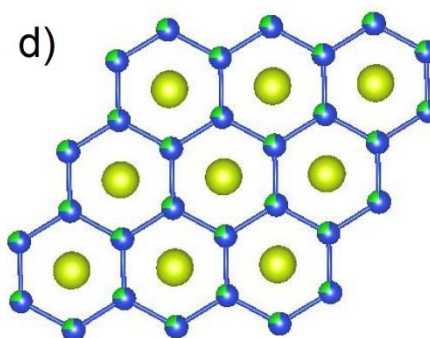


Fig. 1 Crystal structure of three related compounds: (a, b) AlB_2 – small and large balls are boron and aluminum; (c) Ca_2PdGe_3 – large balls represent calcium, small red and blue balls are palladium and germanium; (d) Tb_2PdGe_3 big balls are terbium, small represents palladium and germanium, which occupy hexagonal site with probability 1:3

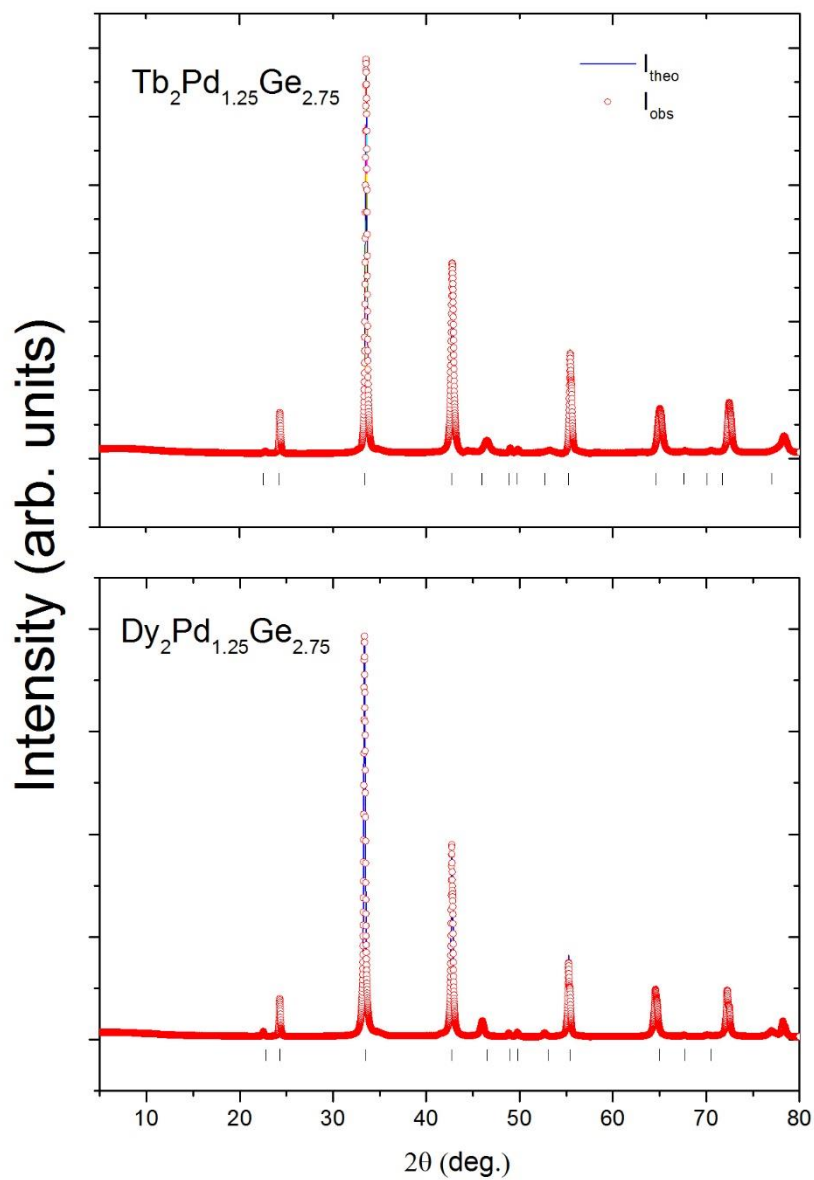


Fig. 2 Le Bail refinement of powder XRD data for $\text{Tb}_2\text{Pd}_{1.25}\text{Ge}_{2.75}$ and $\text{Dy}_2\text{Pd}_{1.25}\text{Ge}_{2.75}$. Observed data and calculated intensity are represented by red circles and blue lines respectively. Black vertical ticks correspond to Bragg peaks for space group P6/mmm (no. 191)

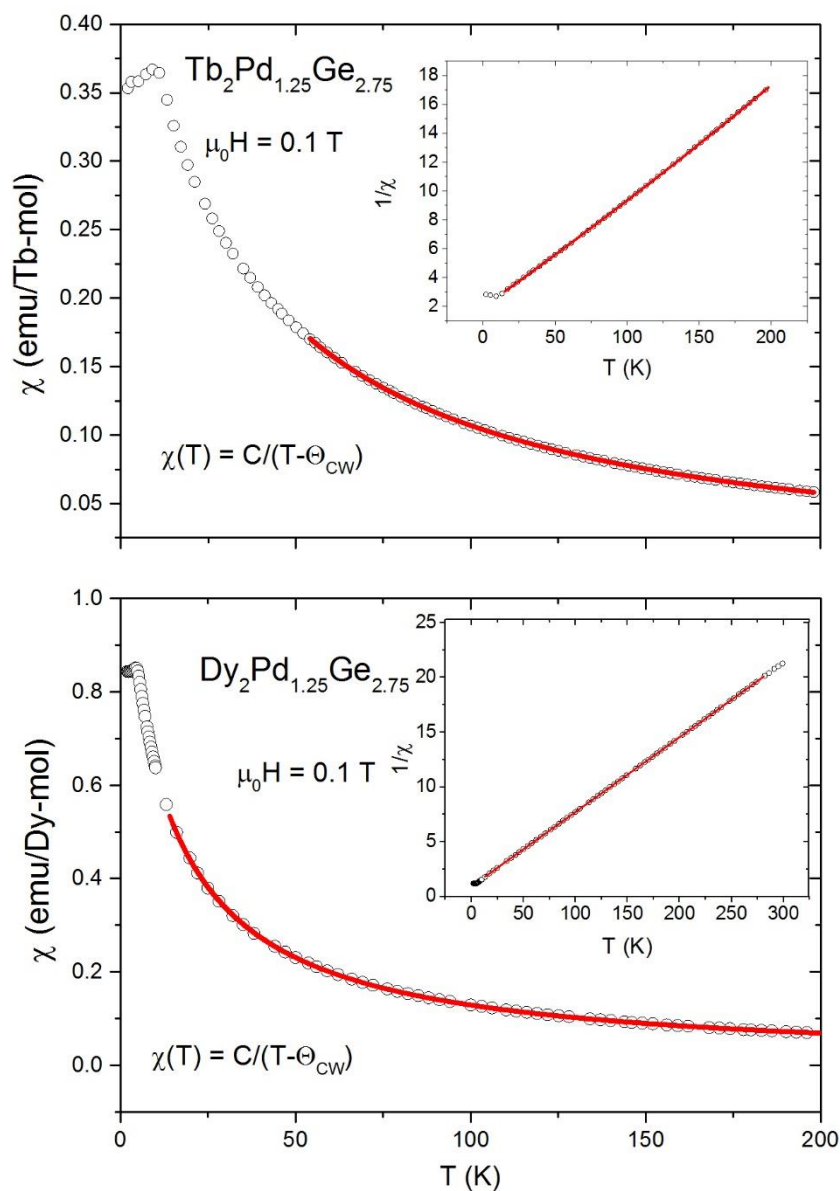


Fig. 3 The temperature dependence of the magnetic susceptibility for $\text{Tb}_2\text{Pd}_{1.25}\text{Ge}_{2.75}$ and $\text{Dy}_2\text{Pd}_{1.25}\text{Ge}_{2.75}$. The red line is a fit to a Curie – Weiss law for temperatures above 50 K and 25 K respectively. The inset shows the inverse magnetic susceptibility as a function of temperature with the fitted function $1/\chi = T/C - \theta_{cw}/C$ (red line).



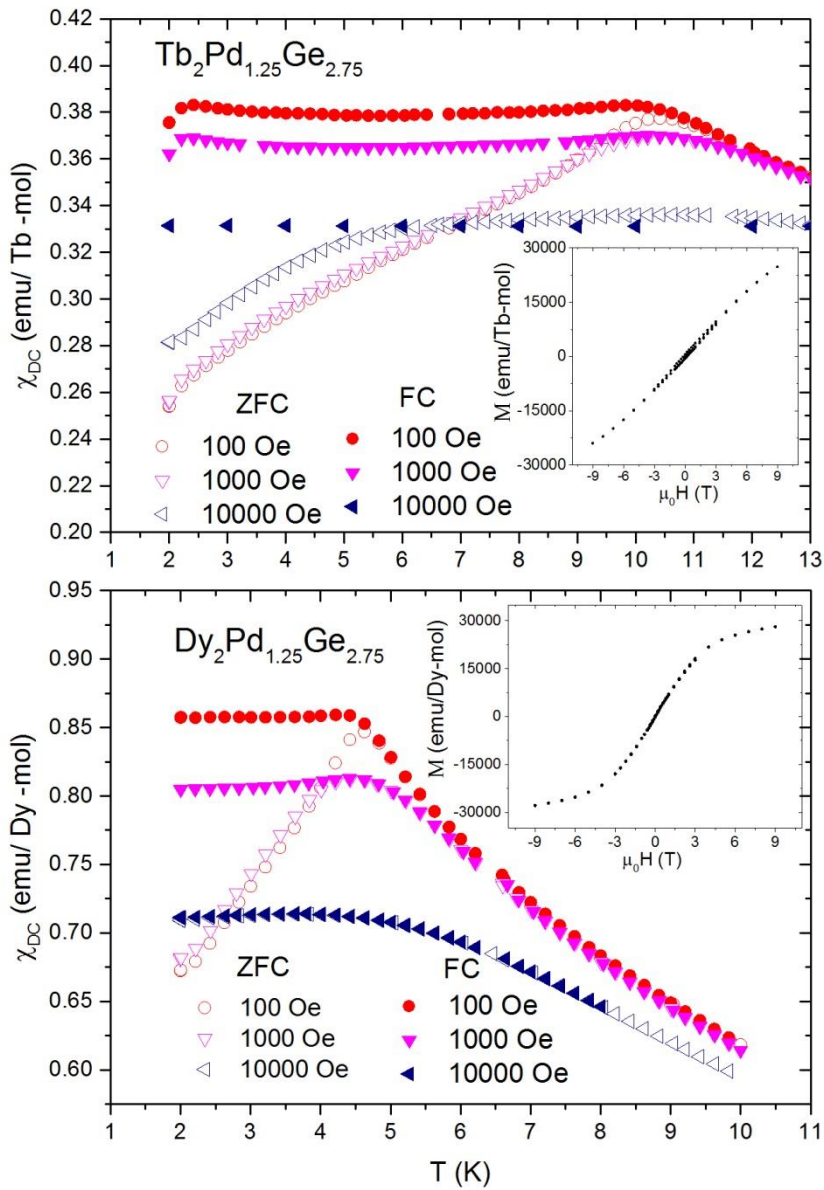


Fig. 4 The difference between ZFC and FC magnetic susceptibility of $\text{Tb}_2\text{Pd}_{1.25}\text{Ge}_{2.75}$ and $\text{Dy}_2\text{Pd}_{1.25}\text{Ge}_{2.75}$ in various values of applied magnetic field. Insets shows $M(H)$ curves for $\text{Tb}_2\text{Pd}_{1.25}\text{Ge}_{2.75}$ and $\text{Dy}_2\text{Pd}_{1.25}\text{Ge}_{2.75}$ at 2 K.

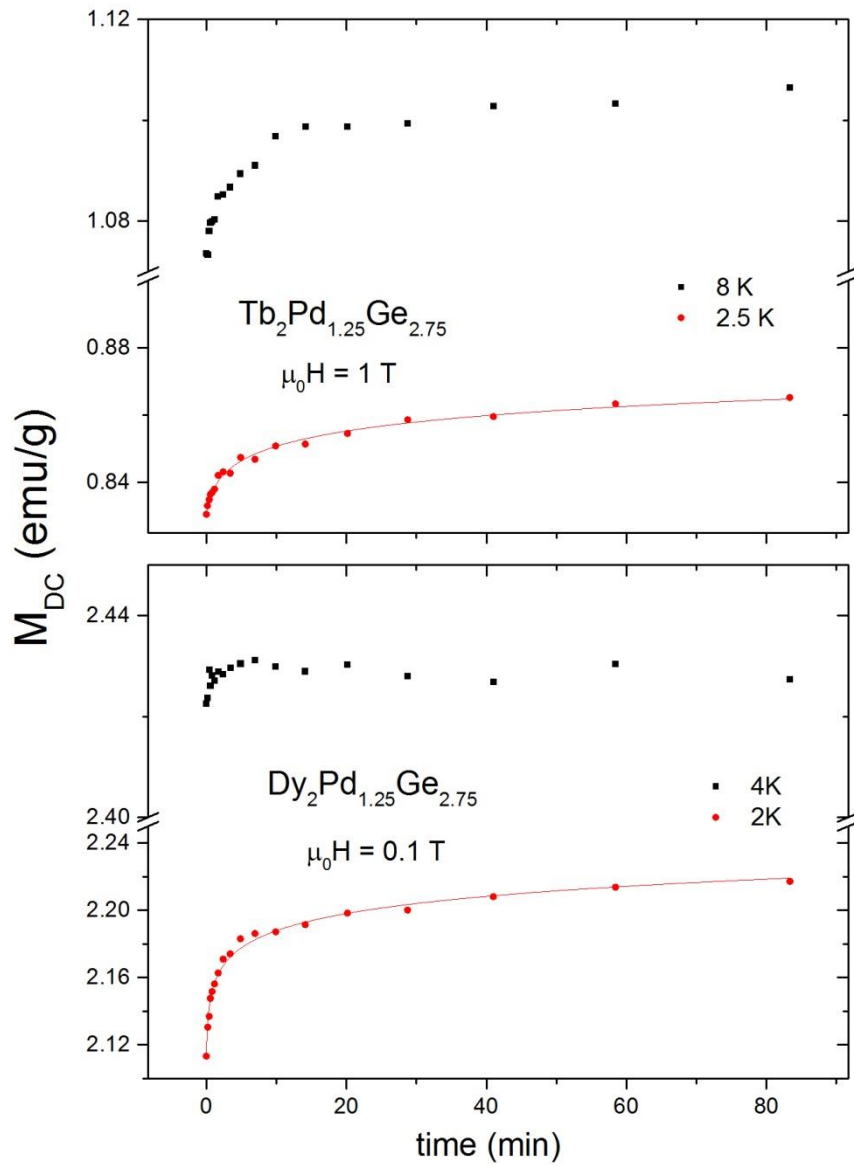


Fig. 5 Time dependent remnant magnetization behavior for $Tb_2Pd_{1.25}Ge_{2.75}$ and $Dy_2Pd_{1.25}Ge_{2.75}$. Solid lines represent fits to equation $M(t) = M_0 + S \ln(t/t_0 + 1)$.

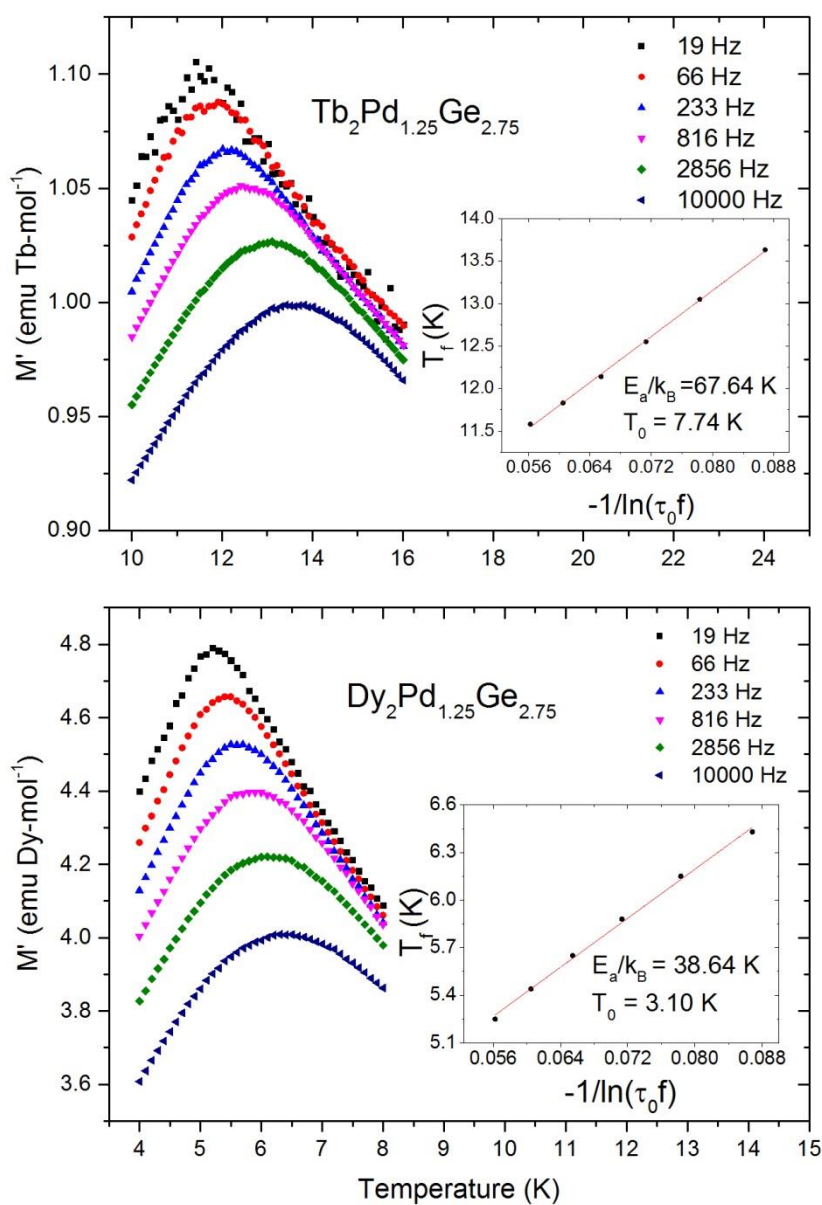


Fig. 6 Temperature dependence of the real part of the ac magnetic susceptibility χ' (T) for $Tb_2Pd_{1.25}Ge_{2.75}$ and $Dy_2Pd_{1.25}Ge_{2.75}$. Insets show plots of the freezing temperature (T_f) versus $1/\ln(\tau_0 f)$ with a Vogel-Fulcher law fit (red solid line).

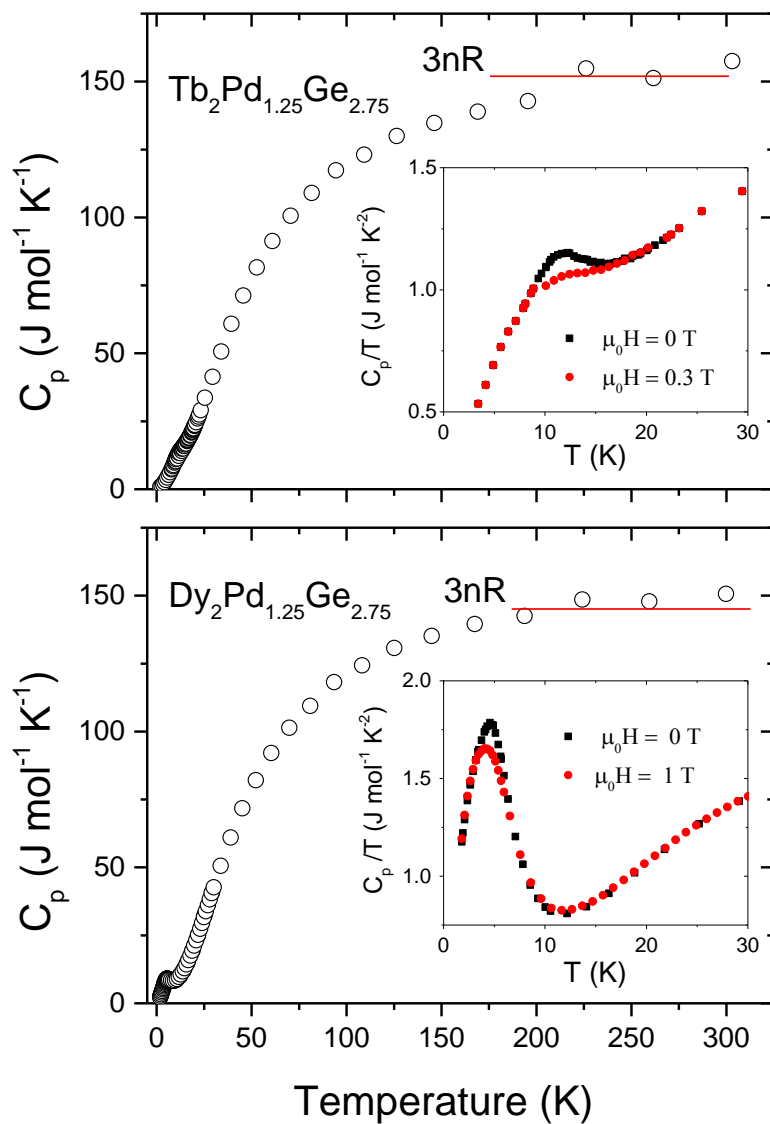


Fig. 7 Temperature dependence of the heat capacity (C_p) for $\text{Tb}_2\text{Pd}_{1.25}\text{Ge}_{2.75}$ and $\text{Dy}_2\text{Pd}_{1.25}\text{Ge}_{2.75}$. Insets show plots of C_p/T vs. T at low temperatures measured with and without applied magnetic field.

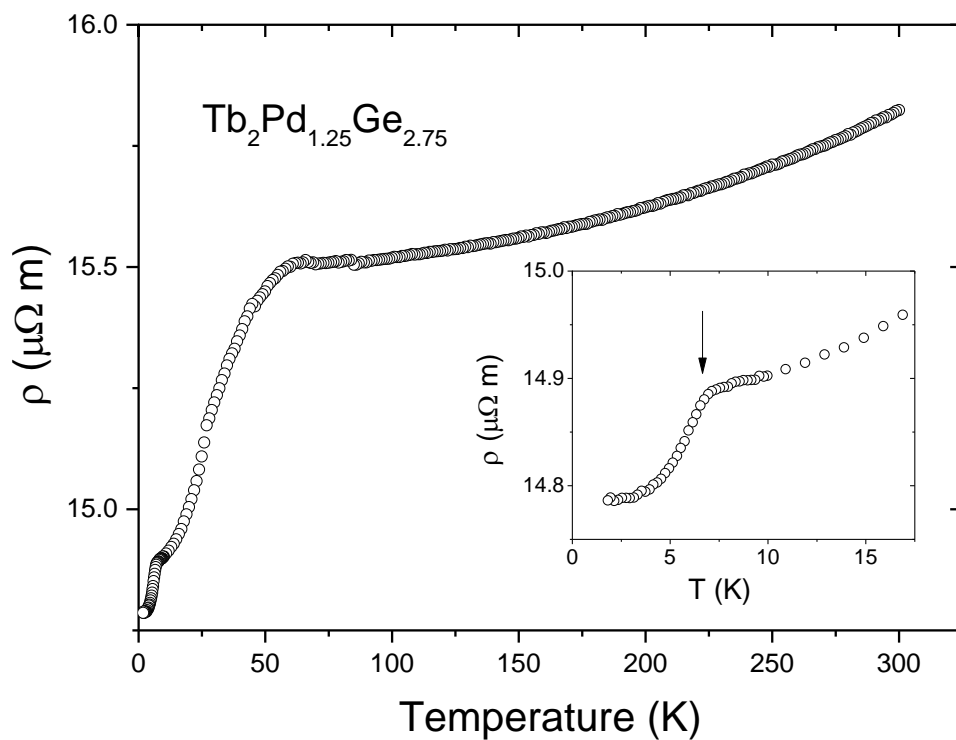


Fig. 8 Electrical resistivity for $\text{Tb}_2\text{Pd}_{1.25}\text{Ge}_{2.75}$ measured at zero magnetic field. The inset shows the low temperature $\rho(T)$ dependence.

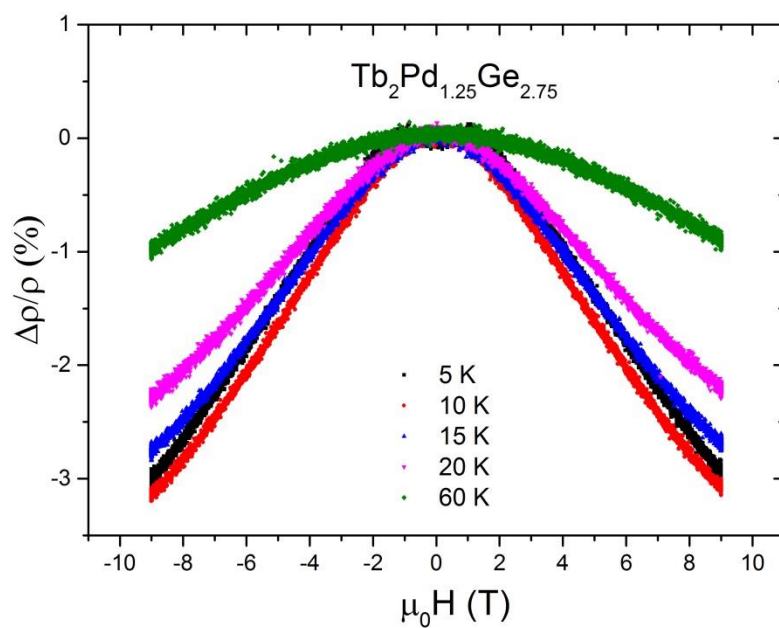


Fig. 9 The magnetoresistance. $\Delta\rho/\rho = [\rho(H) - \rho(0)]/\rho(0)$, as a function of magnetic field for $\text{Tb}_2\text{Pd}_{1.25}\text{Ge}_{2.75}$